ESAIM: PROCEEDINGS, April 2009, Vol. 26, p. 217-229
H. Ammari, Editor

LOCATION SEARCH ALGORITHM OF THIN CONDUCTIVITY INCLUSIONS VIA BOUNDARY MEASUREMENTS

Hyundae Lee[1] and Won-Kwang Park[2]

Abstract. We propose an algorithm for retrieving the end points of thin, rectangular inclusions of finite conductivity in a homogeneous medium proposed herein. It is based on an appropriate asymptotic formula for steady state voltage potentials in the presence of thin inclusions. Numerical experiments exhibit the proposed algorithm is fast, effective and stable.

Introduction

We consider reconstructing end-points of thin conductivity inclusions which occurs in the Electrical Impedance Tomography (EIT). Based on the two-dimensional location search algorithm [6] and asymptotic formula for steady state voltage potentials in the presence of thin inclusions [7], an algorithm for finding the end-points of thin inclusion of discontinuous electrical conductivity by two-different current-voltage measurements has been suggested in [2] and [3] for the single and multiple case respectively.

In this paper, we propose a useful algorithm for retrieving end points of thin inclusions based on an appropriate asymptotic formula for steady state voltage potentials in the presence of thin inclusions. The main idea of this algorithm is to solve the problem of identifying simple poles and residues of a meromorphic function from the measured data on the boundary, the simple poles being the end-points of inclusions and the residues indicates the directions of inclusions for joining end-points.

This paper is structured as follows. In the second section, following this introduction, we introduce the representation formula for the steady state voltage potential in terms of the thickness of inclusions. Then, in section 2, we devoted to the design of algorithm for identifying the end-points. In the last section, we present numerical experiments for demonstrating the performance of proposed algorithm.

1. Representation formula

Let $\Omega \subset \mathbb{R}^2$ be a smooth, bounded domain that represents a homogeneous medium. We assume that this medium contains a set of N well-separated thin inclusions denoted as

$$\Gamma = \bigcup_{j=1}^{N} \Gamma_j$$

[1] Department of Mathematics, Inha University, 253 Yonghyun-dong, Nam-gu, Incheon 402-751, Korea.

[2] Département de Recherche en Électromagnétisme - Laboratoire des Signaux et Systèmes (UMR 8506, CNRS-Supélec-Université Paris-Sud 11) 91192 Gif-sur-Yvette cedex, France.

Article published by EDP Sciences and available at http://www.edpsciences.org/proc or http://dx.doi.org/10.1051/proc/2009015

where each Γ_j are apart from $\partial\Omega$ and localized in the neighborhood of a curve, say γ_j, that is

$$\Gamma_j = \{x + \eta n_j(x) : x \in \gamma_j,\ \eta \in (-\varepsilon, \varepsilon)\},$$

where the supporting σ_j is a straight line in Ω (with strictly positive distance from its boundary $\partial\Omega$, if there were any at finite distance), $n_j(x)$ is the unit normal to γ_j at x, and ε is a positive constant which specifies the thickness of the inclusion (See figure 1).

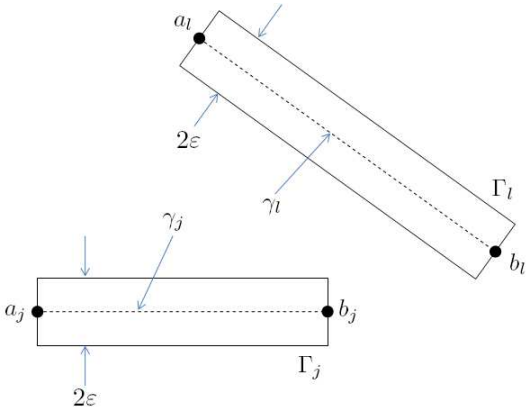

FIGURE 1. Sketch of set of thin inclusions Γ.

Let $0 < \sigma_0 < +\infty$ and $0 < \sigma_j < +\infty$ denote the conductivity of the domain Ω and Γ_j, respectively. Throughout this chapter, we assume that these are strictly positive constants. By using this notation, we adopt the piecewise constant conductivity

$$\sigma(x) = \begin{cases} \sigma_0 & \text{for} \quad x \in \Omega \backslash \overline{\Gamma} \\ \sigma_j & \text{for} \quad x \in \Gamma_j \end{cases} . \tag{1}$$

Throughout this paper, for the sake of simplify, we set σ_0 is equal to 1.

Let u be the steady state voltage potential in the presence of the inclusion Γ, that is, the unique solution to

$$\nabla \cdot \left(\left(1 + \sum_{j=1}^{N} (\sigma_j - 1)\chi_{\Gamma_j} \right) \nabla u(x) \right) = 0 \quad \text{for} \quad x \in \Omega$$

with the Neumann boundary condition

$$\frac{\partial u(x)}{\partial \nu(x)} = g(x) \quad \text{for} \quad x \in \partial\Omega$$

where $\nu(x)$ is unit outward vector on $\partial\Omega$, and the compatibility condition

$$\int_{\partial\Omega} u(x) dS(x) = 0.$$

Here χ_{Γ_j} is the characteristic function of Γ_j, $\nu(x)$ denote the unit outer normal to $\partial\Omega$ at x and the function $g \in H^{-\frac{1}{2}}(\partial\Omega)$ represents the applied boundary current satisfies the compatibility condition

$$\int_{\partial\Omega} g(x) dS(x) = 0.$$

Let us denote u_0 be the potential induced by the current g in the domain Ω without Γ, that is, the unique solution to

$$\Delta u_0(x) = 0 \quad \text{for} \quad x \in \Omega$$

with the Neumann boundary condition

$$\frac{\partial u_0(x)}{\partial \nu(x)} = g(x) \quad \text{for} \quad x \in \partial\Omega$$

and the compatibility condition

$$\int_{\partial\Omega} u_0(x) dS(x) = 0.$$

In order to identify the end points of Γ_j from the collected measurements $u(x)$ on $\partial\Omega$, we will use the following asymptotic expansion of $u(x)$ in terms of the thickness ε (see [7] for a rigorous error analysis and its derivation),

$$\begin{aligned} u(y) &= u_0(y) + \varepsilon u_\gamma(y) \\ &= u_0(y) + \varepsilon \sum_{j=1}^{N} \int_{\gamma_j} \nabla u_0(x) \mathcal{M}^j(x) \nabla_x N(x,y) d\gamma_j(x) + o(\varepsilon), \quad y \in \partial\Omega. \end{aligned} \tag{2}$$

Here $N(x,y)$ is the Neumann function for the domain Ω and $\mathcal{M}^j = (M^j_{kl})_{k,l=1,2}$ is the symmetric matrix defined in appropriate manner as follows :

- $\mathcal{M}^j$ has eigenvectors τ_j and n_j
- The eigenvalue corresponding to τ_j is $2(\sigma_j - 1)$
- The eigenvalue corresponding to n_j is $2\left(1 - \frac{1}{\sigma_j}\right)$.

where τ_j and n_j be unit vectors that are respectively tangent with and normal to γ_j for $j = 1, 2, \cdots, N$.

2. Reconstruction algorithm for identifying the end-points of multiple thin inclusions

In this section, we describe the algorithm for identifying the end-points of multiple thin inclusions. In order to build the algorithm for identifying the end-points, let u_k be the solution with Neumann boundary condition ν_k for $\nu = (\nu_1, \nu_2)$. Let us denote a_j, b_j, $j = 1, \ldots, N$, be the complex numbers representing the end points of thin inclusions and introduce $v(x) = (x_1 + ix_2)^n$ where $x = (x_1, x_2) \in \overline{\Omega}$. Then we have

$$\begin{aligned} \int_{\partial\Omega} (u_k(y) - y_k) \frac{\partial v(y)}{\partial \nu(y)} dS(y) &= \varepsilon \sum_{j=1}^{N} \int_{\partial\Omega} \int_{\gamma_j} (M^j_{k1}, M^j_{k2}) \nabla_x N(x,y) d\gamma_j(x) \frac{\partial v(y)}{\partial \nu(y)} dS(y) + o(\varepsilon) \\ &= \varepsilon \sum_{j=1}^{N} \int_{\gamma_j} (M^j_{k1}, M^j_{k2}) \nabla v(x) d\gamma_j(x) + o(\varepsilon) \\ &= \varepsilon \sum_{j=1}^{N} (M^j_{k1} + iM^j_{k2}) \frac{|b_j - a_j|}{b_j - a_j} (b_j^n - a_j^n) + o(\varepsilon). \end{aligned}$$

By using two different boundary measurements u_1 and u_2, we can obtain

$$\begin{aligned}\int_{\partial\Omega}[u_1(y)-y_1-i(u_2(y)-y_2)]\frac{\partial}{\partial\nu(y)}(y_1+iy_2)^n dS(y)\\ =\varepsilon\sum_{j=1}^{N}\mathrm{trace}(\mathcal{M}^j)\frac{\overline{b_j-a_j}}{|b_j-a_j|}(b_j^n-a_j^n)+o(\varepsilon)\end{aligned}\tag{3}$$

here $\mathrm{trace}(\mathcal{M}^j)$ is the trace of matrix $\mathcal{M}^j$ for $j=1,2,\cdots,N$. Combining (3) with the Simple Pole Algorithm [9], we can construct the following reconstruction algorithm.

Step 1 Set $c_0=0$. For sufficiently large M, let us calculate the complex numbers c_n for $n=1,2,\cdots,2M-1$, by

$$c_n:=\int_{\partial\Omega}[u_1(y)-y_1-i(u_2(y)-y_2)]\frac{\partial}{\partial\nu(y)}(y_1+iy_2)^n dS(y).\tag{4}$$

Step 2 Solve for $l_1,l_2,\cdots,l_M$ the system of linear equations

$$\begin{pmatrix}c_0 & c_1 & \cdots & c_{M-1}\\ c_1 & c_2 & \cdots & c_M\\ \vdots & \vdots & & \vdots\\ c_{M-1} & c_M & \cdots & c_{2M-2}\end{pmatrix}\begin{pmatrix}l_M\\ l_{M-1}\\ \vdots\\ l_1\end{pmatrix}=\begin{pmatrix}-c_M\\ -c_{M+1}\\ \vdots\\ -c_{2M-1}\end{pmatrix}.\tag{5}$$

Step 3 (Determination of end-points) Find the zeros $\alpha_1,\alpha_2,\cdots,\alpha_M$ of the polynomial equation

$$z^M+l_1z^{M-1}+\cdots+l_M=0.$$

Step 4 (Determination of residue for joining end-points) Solve the equation

$$\begin{pmatrix}1 & 1 & \cdots & 1\\ \alpha_1 & \alpha_2 & \cdots & \alpha_N\\ \vdots & \vdots & & \vdots\\ \alpha_1^{M-1} & \alpha_2^{M-1} & \cdots & \alpha_M^{M-1}\end{pmatrix}\begin{pmatrix}\beta_1\\ \beta_2\\ \vdots\\ \beta_M\end{pmatrix}=\begin{pmatrix}c_0\\ c_1\\ \vdots\\ c_{M-1}\end{pmatrix}$$

to find $\beta_1,\beta_2,\cdots,\beta_M$.

Step 5 Finally, discard α_j if $|\beta_j|$ is reasonably small. To find the line segments, join the remaining α_j's with the same corresponding β's up to sign. If it is not enough, then consider also the directions of β's.

3. Numerical examples

In this section, the numerical simulations for identifying end-points of multiple thin inclusions are considered, according to the algorithm introduced in the previous section 2. The domain Ω is chosen as a unit disk centered at $(0,0)$ in $\mathbb{R}^2$ and the thickness ε of all thin inclusions Γ_j is 0.02. As we mentioned in section 1, we first adopt a rectangular shape of the thin inclusions due to the stability of algorithm. For the first example, we consider the case of two thin inclusions parameterized as

$$\Gamma_j=\{x+\eta n_j(x):x\in\gamma_j,\ \eta\in(-\varepsilon,\varepsilon)\},$$

where

$$\begin{aligned}\gamma_1&=\left\{\left(z,\frac{0.2(z-0.3464)}{0.3464}+0.2\right):z\in(-0.3464,0.3464)\right\}\\ \gamma_2&=\{(z,-0.4):z\in(-0.4,0.3)\}\end{aligned}$$

and the parameter σ_j is chosen as 5 for $j = 1, 2$. Notice that the end-points of Γ_1 are

$$a_1 = (0.3464, 0.2000) \quad \text{and} \quad b_1 = (-0.3464, -0.2000)$$

and the end-points of Γ_2 are

$$a_2 = (0.3000, -0.4000) \quad \text{and} \quad b_2 = (-0.4000, -0.4000).$$

$\lvert\beta_j\rvert$	β_j	α_j	End-Points
0.0000	$-0.0000 - 0.0000i$	$-0.0296 - 1.6380i$	No
0.0000	$-0.0000 - 0.0000i$	$1.5328 - 0.0336i$	No
0.0000	$-0.0000 - 0.0000i$	$0.7049 + 1.4487i$	No
0.0000	$-0.0000 - 0.0000i$	$-0.3909 + 1.2754i$	No
0.0000	$-0.0000 - 0.0000i$	$-1.2169 + 0.2539i$	No
0.1836	$0.1809 - 0.0314i$	$-0.3701 - 0.4040i$	Yes
0.0935	$0.0822 - 0.0447i$	$-0.3719 - 0.1834i$	Yes
0.1636	$-0.1611 - 0.0285i$	$0.2900 - 0.4165i$	Yes
0.1685	$-0.1505 + 0.0759i$	$0.3423 + 0.1913i$	Yes
0.0563	$0.0484 + 0.0287i$	$0.1821 - 0.0272i$	No

TABLE 1. Computed values of α_j, β_j and $|\beta_j|$ for the first example without noise.

In order to find the end-points of those two thin inclusions, we have performed the reconstruction presented in previous section with the value of $M = 10$. Obtained values of α_j, β_j and $|\beta_j|$ are illustrated in Table 1. From this information, we discard α_j when the associated value of $|\beta_j|$ is too small and we find four end-points of two thin inclusions.

$\lvert\beta_j\rvert$	β_j	α_j	End-Points
0.0000	$-0.0000 - 0.0000i$	1.6858 + 0.3455i	No
0.0000	$-0.0000 - 0.0000i$	$-0.5717 - 1.4782i$	No
0.0000	$-0.0000 + 0.0000i$	$0.1228 + 1.0485i$	No
0.0000	$0.0000 - 0.0000i$	$-0.5925 + 0.9217i$	No
0.0000	$0.0000 - 0.0000i$	$-1.0739 + 0.1080i$	No
0.1607	$-0.1348 + 0.0874i$	$0.3373 + 0.2012i$	Yes
0.0586	$-0.0584 + 0.0040i$	$0.3546 - 0.3604i$	No
0.0891	$-0.0888 - 0.0074i$	$0.2940 - 0.4526i$	Yes
0.1398	$0.1398 + 0.0003i$	$-0.3879 - 0.4139i$	Yes
0.1653	$0.1422 - 0.0843i$	$-0.3364 - 0.2337i$	Yes

TABLE 2. Computed values of α_j, β_j and $|\beta_j|$ for the first example with $\xi = 10^{-5}$.

Let us assume that some noise is added to the measured boundary data, i.e., for $x \in \partial\Omega$

$$u_{\text{noise}}(x) = u(x) + \xi \times \text{rnd}(-1, 1)$$

where $\text{rnd}(-1, 1)$ is a arbitrary real value between -1 and 1. Table 2, for the case $\xi = 10^{-5}$, shows that the algorithm detects end-points and residues accurately. Notice that higher noise level (greater than $\xi = 10^{-5}$) leads to poor results (we observe that the value of α_j is poor). We recommend [9] for a more detailed discussion.

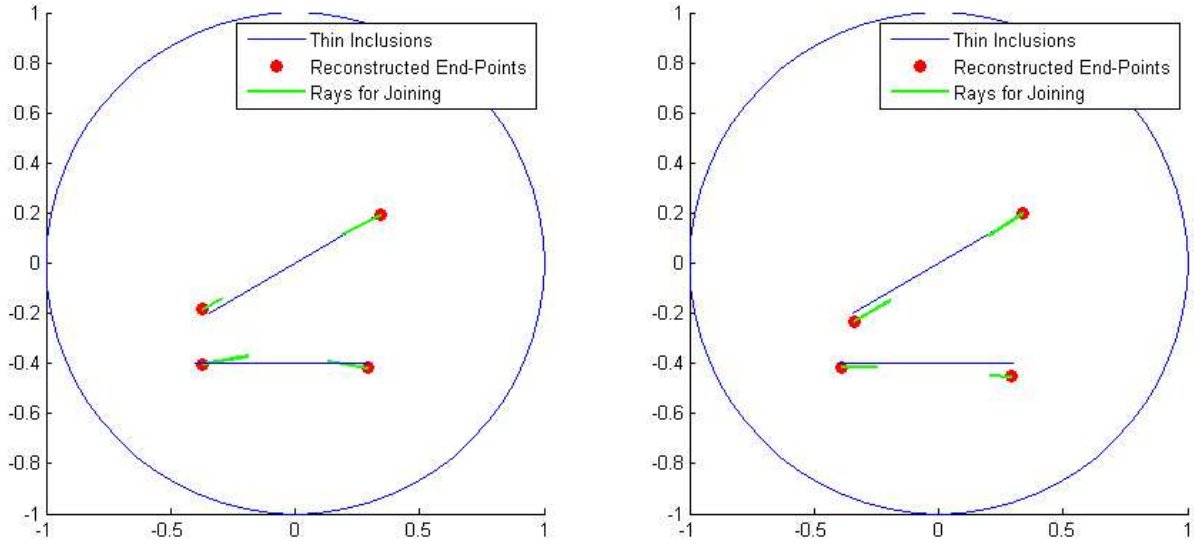

FIGURE 2. Reconstructions of two thin inclusions. γ_j's are given blue lines. Red circles and green rays starting from them represent α_j and $\overline{\beta_j}$ without noise (left) and some noise $\xi = 10^{-5}$ (right).

In figure 2, we illustrate the results. From them, we can conclude that we retrieve the expected end-points of thin inclusions.

Next, we consider the case of three thin inclusions parameterized as

$$\Gamma_j = \{x + \eta n_j(x) : x \in \gamma_j,\ \eta \in (-\varepsilon, \varepsilon)\},$$

where

$$\gamma_1 = \left\{ \left(z, -\frac{0.5656(z - 0.6822)}{0.5650} - 0.2828 \right) : z \in (0.1172, 0.6822) \right\}$$
$$\gamma_2 = \{(z, -0.5) : z \in (-0.6, 0.2)\}$$
$$\gamma_3 = \left\{ \left(z, -\frac{0.7608(z + 0.5236)}{0.2472} + 0.0196 \right) : z \in (-0.5236, -0.2764) \right\}$$

and the parameter σ_j is chosen as 5 for $j = 1, 2, 3$. Notice that the end-points of Γ_1 are

$$a_1 = (0.1172, 0.2828) \quad \text{and} \quad b_1 = (0.6822, -0.2828)$$

the end-points of Γ_2 are

$$a_2 = (-0.6000, -0.5000) \quad \text{and} \quad b_2 = (0.2000, -0.5000)$$

and the end-points of Γ_3 are

$$a_3 = (-0.5236, 0.0196) \quad \text{and} \quad b_3 = (-0.2764, 0.7804).$$

The reconstruction algorithm with the value of $M = 10$ yields values of α_j, β_j and $|\beta_j|$ illustrated in Table 3. Again, we discard α_j when the associated value of $|\beta_j|$ is small and we find six end-points of three thin inclusions.

$\lvert\beta_j\rvert$	β_j	α_j	End-Points
0.0000	$-0.0000 - 0.0000i$	$3.8899 - 3.0467i$	No
0.0000	$-0.0000 - 0.0000i$	$1.4003 + 1.1729i$	No
0.0002	$-0.0000 - 0.0002i$	$-0.4983 - 0.8912i$	No
0.1638	$-0.1168 - 0.1148i$	$0.6850 - 0.2789i$	Yes
0.1830	$0.1830 - 0.0046i$	$-0.5917 - 0.5000i$	Yes
0.1354	$-0.1352 + 0.0086i$	$0.2146 - 0.5150i$	Yes
0.0212	$0.0156 - 0.0144i$	$-0.3873 + 0.7603i$	No
0.1810	$-0.0739 + 0.1652i$	$-0.2789 + 0.7669i$	Yes
0.2170	$0.0565 - 0.2095i$	$-0.4898 + 0.0250i$	Yes
0.1839	$0.0708 + 0.1698i$	$0.1654 + 0.2345i$	Yes

TABLE 3. Computed values of α_j, β_j and $|\beta_j|$ for the second example without noise.

In contrast with the previous example, table 4, for the case $\xi = 10^{-4}$, shows that the algorithm detects end-points and residues accurately.

$\lvert\beta_j\rvert$	β_j	α_j	End-Points
0.0000	$0.0000 - 0.0000i$	$0.6439 + 1.4667i$	No
0.0003	$0.0003 - 0.0000i$	$-0.1765 + 1.0658i$	No
0.0017	$0.0016 - 0.0005i$	$0.6953 - 0.5859i$	No
0.1459	$-0.1080 - 0.0981i$	$0.6953 - 0.2751i$	Yes
0.1530	$-0.0507 + 0.1444i$	$-0.2767 + 0.7864i$	Yes
0.0922	$-0.0887 - 0.0252i$	$0.1764 - 0.5697i$	Yes
0.2028	$0.2028 - 0.0049i$	$-0.5851 - 0.4936i$	Yes
0.0124	$0.0036 - 0.0119i$	$-0.6685 + 0.2048i$	No
0.2327	$0.0067 - 0.2326i$	$-0.4883 - 0.0521i$	Yes
0.2311	$0.0324 + 0.2288i$	$0.1888 + 0.1661i$	Yes

TABLE 4. Computed values of α_j, β_j and $|\beta_j|$ for the second example with $\xi = 10^{-4}$.

In figure 3, we illustrate the results. We can say that we have obtained the expected end-points of the thin inclusions.

Let us examine the effect of the value σ_j's. To observe this, we have performed the numerical simulations under the same condition as the one of the second example except σ_j's. The parameter σ_j is chosen as $\sigma_1 = 10$, $\sigma_2 = 5$, and $\sigma_3 = 20$.

The reconstruction algorithm is applied with the value of $M = 10$. The obtained values of α_j, β_j and $|\beta_j|$ are illustrated in table 5. We still discard α_j when the associated value of $|\beta_j|$ is small and we find six end-points of the three thin inclusions.

From the results illustrated in figure 4, we can easily observe that the algorithm is not sensitive to the values of σ_j, neither to translation and rotation of the thin inclusions. Moreover, the rays starting from the estimated end-points are getting long whenever σ_j is large (and getting short for small σ_j), i.e., we can easily join the end-points.

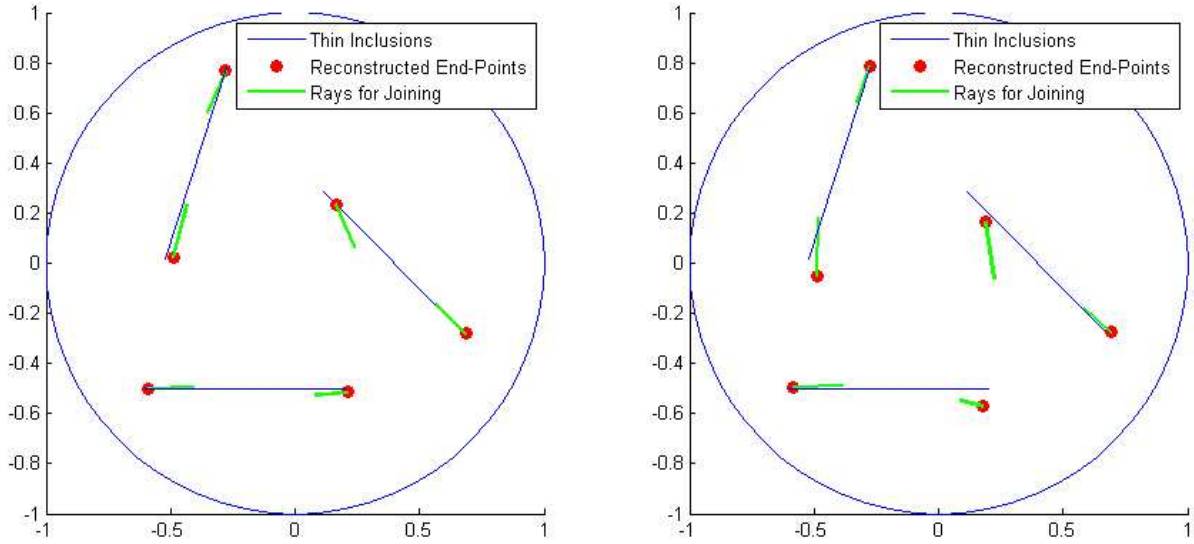

FIGURE 3. (All σ_j are same.) Reconstructions of three thin inclusions. γ_j's are given blue lines. Red circles and green rays starting from them represent α_j and $\overline{\beta_j}$ without noise (left) and some noise $\xi = 10^{-4}$ (right).

$\lvert\beta_j\rvert$	β_j	α_j	End-Points
0.0000	$-0.0000 - 0.0000i$	$1.1281 + 0.8499i$	No
0.0000	$-0.0000 - 0.0000i$	$-0.0730 - 1.2244i$	No
0.2622	$-0.1816 - 0.1892i$	$0.6808 - 0.2786i$	Yes
0.0002	$-0.0001 - 0.0000i$	$-0.9143 - 0.4280i$	No
0.1081	$-0.1065 - 0.0186i$	$0.1960 - 0.5422i$	Yes
0.1940	$0.1940 - 0.0018i$	$-0.5865 - 0.4953i$	Yes
0.4325	$-0.1154 + 0.4168i$	$-0.2888 + 0.7606i$	Yes
0.0469	$-0.0279 - 0.0377i$	$-0.4103 + 0.7103i$	No
0.5314	$0.1125 - 0.5194i$	$-0.4791 + 0.0255i$	Yes
0.3717	$0.1251 + 0.3500i$	$0.1608 + 0.1875i$	Yes

TABLE 5. Computed values of α_j, β_j and $\lvert\beta_j\rvert$ for the third example without noise.

Now, we apply the algorithm to the non-rectangular thin inclusions. For the fourth example, we consider the case of two thin inclusions parameterized as

$$\Gamma_j = \{x + \eta n_j(x) : x \in \gamma_j,\ \eta \in (-\varepsilon, \varepsilon)\},$$

where

$$\gamma_1 = \left\{(z, (z+0.2)^2 + 0.3), z \in (-0.7.0.3)\right\}$$
$$\gamma_2 = \left\{(z, -(z-0.2)^2 - 0.3), z \in (-0.3.0.7)\right\}$$

$\lvert\beta_j\rvert$	β_j	α_j	End-Points
0.0000	$0.0000 + 0.0000i$	$0.5984 - 1.1642i$	No
0.0002	$0.0001 + 0.0002i$	$0.6639 + 0.6711i$	No
0.2613	$-0.1821 - 0.1874i$	$0.6810 - 0.2778i$	Yes
0.1011	$-0.1007 - 0.0094i$	$0.2054 - 0.5468i$	Yes
0.1870	$0.1870 + 0.0048i$	$-0.5916 - 0.4962i$	Yes
0.0001	$-0.0000 - 0.0001i$	$-0.9788 + 0.1254i$	No
0.0150	$-0.0037 - 0.0145i$	$-0.4584 + 0.7498i$	No
0.4052	$-0.1359 + 0.3817i$	$-0.2826 + 0.7621i$	Yes
0.5505	$0.1683 - 0.5241i$	$-0.4697 + 0.0393i$	Yes
0.3553	$0.0671 + 0.3490i$	$0.1805 + 0.1636i$	Yes

TABLE 6. Computed values of α_j, β_j and $|\beta_j|$ for the third example with $\xi = 10^{-4}$.

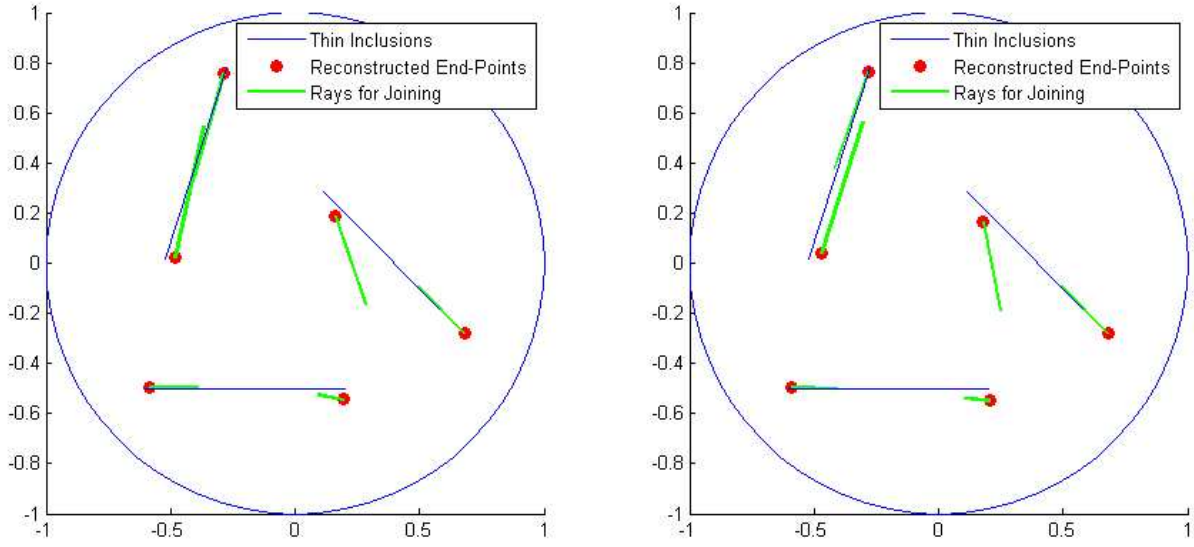

FIGURE 4. (All σ_j are different.) Reconstructions of three thin inclusions. γ_j's are given blue lines. Red circles and green rays starting from them represent α_j and $\overline{\beta_j}$ without noise (left) and some noise $\xi = 10^{-4}$ (right).

and the parameter σ_j is chosen as 5 for $j = 1, 2$. Notice that the end-points of Γ_1 are

$$a_1 = (-0.7000, 0.5500) \quad \text{and} \quad b_1 = (0.3000, 0.5500)$$

and the end-points of Γ_2 are

$$a_2 = (-0.3000, -0.5500) \quad \text{and} \quad b_2 = (0.7000, -0.5500).$$

Typical results are in table 7, 8 and figure 5 with the value of $M = 10$ and $\xi = 5 \times 10^{-4}$. At this stage, to retrieve the end-points, we must join the α's with the same corresponding β's up to sign of real part, i.e., choose β_j and β_l that satisfy $\beta_j \approx -\overline{\beta}_l$.

$\lvert\beta_j\rvert$	β_j	α_j	End-Points
0.0000	$0.0000 + 0.0000i$	$-0.8850 - 1.3360i$	No
0.0000	$-0.0000 - 0.0000i$	$0.5600 + 0.8748i$	No
0.1269	$-0.0981 - 0.0804i$	$0.7038 - 0.5544i$	Yes
0.1341	$-0.1190 + 0.0617i$	$0.3082 + 0.5307i$	Yes
0.1253	$0.0953 + 0.0814i$	$-0.6682 + 0.5271i$	Yes
0.0571	$0.0462 - 0.0336i$	$-0.5671 + 0.3783i$	No
0.1309	$0.1142 - 0.0641i$	$-0.2906 - 0.5200i$	Yes
0.0847	$-0.0655 + 0.0538i$	$0.5206 - 0.3426i$	No
0.0841	$0.0618 + 0.0571i$	$0.2073 - 0.3395i$	No
0.0834	$-0.0347 - 0.0758i$	$-0.2507 + 0.1599i$	No

TABLE 7. Computed values of α_j, β_j and $|\beta_j|$ for the fourth example without noise.

$\lvert\beta_j\rvert$	β_j	α_j	End-Points
0.0000	$-0.0000 + 0.0000i$	$1.2877 + 0.7279i$	No
0.0000	$-0.0000 - 0.0000i$	$-1.1314 - 0.4502i$	No
0.0885	$-0.0769 - 0.0438i$	$0.7226 - 0.5681i$	Yes
0.0512	$-0.0510 - 0.0042i$	$0.7210 - 0.4121i$	No
0.0072	$0.0034 - 0.0064i$	$-0.1419 - 0.8116i$	No
0.0694	$0.0655 - 0.0230i$	$-0.3880 - 0.5647i$	Yes
0.1007	$-0.0955 + 0.0318i$	$0.3505 + 0.5516i$	Yes
0.0005	$-0.0005 + 0.0001i$	$-0.9437 + 0.4924i$	No
0.1488	$0.1362 + 0.0600i$	$-0.6774 + 0.5015i$	Yes
0.0238	$0.0188 - 0.0145i$	$-0.2383 + 0.5702i$	No

TABLE 8. Computed values of α_j, β_j and $|\beta_j|$ for the fourth example with $\xi = 5 \times 10^{-4}$.

For last example, we consider the case of two thin inclusions parameterized as

$$\Gamma_j = \{x + \eta n_j(x) : x \in \gamma_j,\ \eta \in (-\varepsilon, \varepsilon)\},$$

where

$$\gamma_1 = \left\{(z, -0.5(z-0.2)^2 + 0.5) : z \in (-0.7, 0.3)\right\}$$
$$\gamma_2 = \left\{(z, (z-0.2)^3 + (z-0.2)^2) - 0.4 : z \in (-0.3, 0.7)\right\}$$

and the parameter σ_j is chosen as 10 and 5 for $j = 1$ and 2 respectively. Notice that the end-points of Γ_1 are

$$a_1 = (-0.7000, 0.3750) \quad \text{and} \quad b_1 = (0.3000, 0.3750)$$

and the end-points of Γ_2 are

$$a_2 = (-0.3000, -0.2750) \quad \text{and} \quad b_2 = (0.7000, -0.0250).$$

We exhibit the results in table 9, 10 and in figure 6 with the value of $M = 10$ and $\xi = 10^{-4}$.

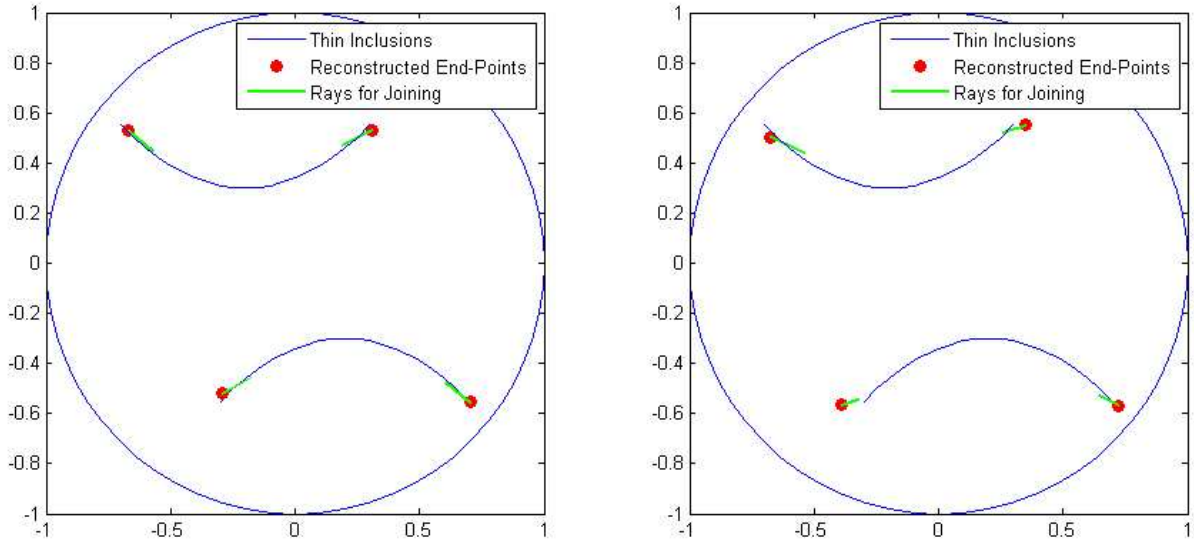

FIGURE 5. Reconstructions of two thin inclusions. γ_j's are given blue lines. Red circles and green rays starting from them represent α_j and $\overline{\beta_j}$ without noise (left) and some noise $\xi = 5 \times 10^{-4}$ (right).

$\lvert\beta_j\rvert$	β_j	α_j	End-Points
0.0000	$-0.0000 - 0.0000i$	$0.4213 + 1.5638i$	No
0.0000	$0.0000 + 0.0000i$	$0.6548 - 1.1992i$	No
0.0000	$-0.0000 + 0.0000i$	$-0.9071 - 0.9568i$	No
0.0013	$-0.0013 + 0.0003i$	$-0.7794 + 0.5024i$	No
0.3108	$0.2997 - 0.0823i$	$-0.6715 + 0.3952i$	Yes
0.1080	$-0.0384 + 0.1010i$	$0.6892 - 0.0122i$	Yes
0.1093	$0.0958 + 0.0526i$	$-0.3267 - 0.2862i$	Yes
0.3343	$-0.1562 - 0.2956i$	$0.2587 - 0.2873i$	No
0.2597	$-0.2167 - 0.1432i$	$0.3112 + 0.3776i$	Yes
0.3677	$0.0170 + 0.3673i$	$-0.1222 + 0.2703i$	No

TABLE 9. Computed values of α_j, β_j and $|\beta_j|$ for the final example without noise.

4. Conclusion

In this article, we propose an algorithm based on the detection of simple poles of a meromorphic function in terms of measured boundary values to retrieve the end-points of thin conductivity inclusions and perform several numerical simulations and it turns out that the proposed algorithm identifies the number and the location of end-points of such thin inclusions accurately.

Our new algorithm offers very useful information and we can say that a good initial guess is obtained at low computational cost, to be improved upon by an appropriate iterative algorithm for example, a level-set evolution [1, 8].

$\lvert\beta_j\rvert$	β_j	α_j	End-Points
0.0000	$0.0000 + 0.0000i$	$-1.4783 - 0.3837i$	No
0.0000	$0.0000 + 0.0000i$	$-0.3574 + 1.1247i$	No
0.0001	$0.0001 - 0.0000i$	$0.9674 + 0.4505i$	No
0.0001	$-0.0001 + 0.0000i$	$0.4970 - 0.8952i$	No
0.3132	$0.2994 - 0.0921i$	$-0.6713 + 0.3913i$	Yes
0.0941	$-0.0360 + 0.0869i$	$0.7011 - 0.0155i$	Yes
0.2972	$-0.2384 - 0.1774i$	$0.3053 + 0.3721i$	Yes
0.0748	$0.0547 + 0.0511i$	$-0.3701 - 0.3052i$	Yes
0.3844	$-0.2338 - 0.3051i$	$0.2732 - 0.2638i$	No
0.4631	$0.1543 + 0.4366i$	$-0.1578 + 0.1843i$	No

TABLE 10. Computed values of α_j, β_j and $|\beta_j|$ for the final example with $\xi = 10^{-4}$.

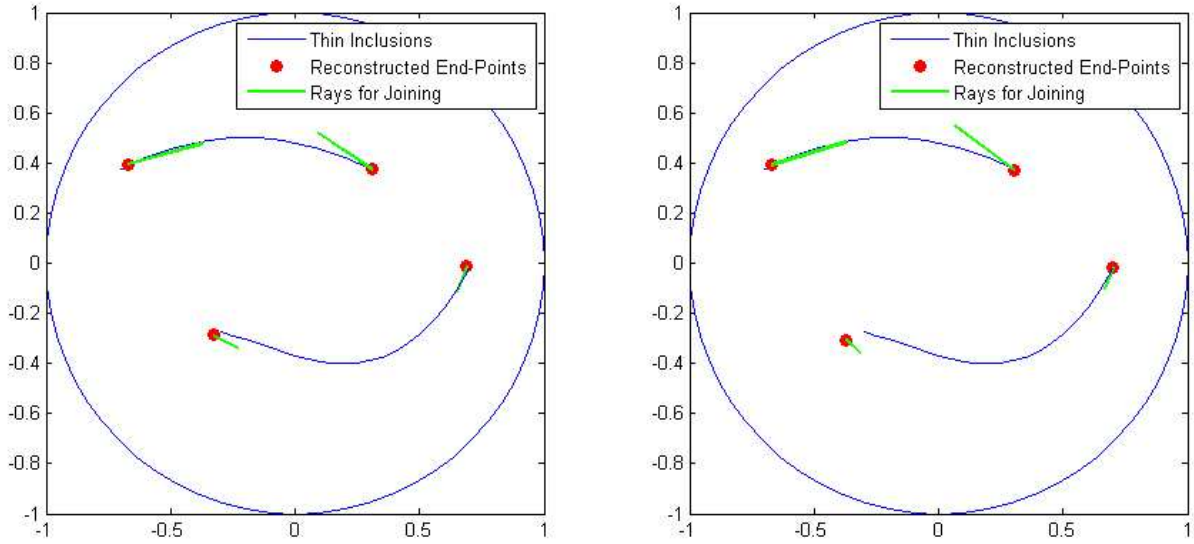

FIGURE 6. (All σ_j are different.) Reconstructions of two thin inclusions. γ_j's are given blue lines. Red circles and green rays starting from them represent α_j and $\overline{\beta_j}$ without noise (left) and some noise $\xi = 10^{-4}$ (right).

The authors [10] suggested an imaging method by the solutions with fixed non-zero high frequency for the imaging of thin inclusions based on the MUSIC (MUltiple SIgnal Classification)-type algorithm. It is still desirable to have an efficient and fast method for imaging of arbitrary shaped thin inclusions using finitely many measurements.

ACKNOWLEDGMENT

The second author would like to acknowledge the careful consideration given to the manuscript by D. Lesselier. Both authors are grateful to H. Ammari for outlining the research topic to them and for his attention to the theoretical issues involved.

References

[1] D. Àlvarez, O. Dorn and M. Moscoso, "Reconstructing thin shapes from boundary electrical measurements with level sets", *Int. J. Informa. Syst. Scie.*, vol. 2, no. 4, pp. 498–511, 2006.

[2] H. Ammari, E. Beretta and E. Francini, "Reconstruction of thin conductivity imperfections", *Applicable Analysis*, vol. 83, pp. 63–78, 2004.

[3] H. Ammari, E. Beretta and E. Francini, "Reconstruction of thin conductivity imperfections, II. The case of multiple segments", *Applicable Analysis*, vol. 85, pp. 87–105, 2006.

[4] H. Ammari and H. Kang, "Reconstruction of small inhomogeneities from boundary measurements", Lecture Notes in Mathematics, Volume 1846, Springer-Verlag, Berlin, 2004.

[5] H. Ammari and H. Kang, "Polarization and moment tensors with applications in inverse problems and effective medium theory", Applied Mathematical Sciences, Volume 162, Springer-Verlag, New York, 2007.

[6] H. Ammari and J. K. Seo, "An accurate formula for the reconstruction of conductivity inhomogeneities", *Advances in Appl. Math.*, vol. 30, pp. 679–750, 2003.

[7] E. Beretta, E. Francini and M. Vogelius, "Asymptotic formulas for steady state voltage potentials in the presence of thin inhomogeneities. A rigorous error analysis", *Journal de Mathématiques Pures et Appliquée*, vol. 82, pp. 1277–1301, 2003.

[8] O. Dorn and D. Lesselier, "Level set methods for inverse scattering", *Inverse Problems*, vol. 22, R67–R131, 2006.

[9] H. Kang and H. Lee, "Identification of simple poles via boundary measurements and an application to EIT", *Inverse Problems*, vol. 20, pp. 1853–1863, 2004.

[10] W. K. Park and D. Lesselier, "MUSIC-type, non-iterative imaging of a thin penetrable inclusion from its far-field multi-static response matrix", *preprint*.